ORIGINAL PAPER

Reforming of CO_2-Containing Natural Gas Using an AC Gliding Arc System: Effects of Operational Parameters and Oxygen Addition in Feed

Nongnuch Rueangjitt · Thammanoon Sreethawong · Sumaeth Chavadej

Abstract   In this research, the reforming of simulated natural gas containing a high CO_2 content under AC non-thermal gliding arc discharge with partial oxidation was conducted at ambient temperature and atmospheric pressure, with specific regards to the concept of the direct utilization of natural gas. This work aimed at investigating the effects of applied voltage and input frequency, as well as the effect of adding oxygen on the reaction performance and discharge stability in the reforming of the simulated natural gas having a CH_4:C_2H_6:C_3H_8:CO_2 molar ratio of 70:5:5:20. The results showed marked increases in both CH_4 conversion and product yield with increasing applied voltage and decreasing input frequency. The selectivities for H_2, C_2H_6, C_2H_4, C_4H_{10}, and CO were observed to be enhanced at a higher applied voltage and at a lower frequency, whereas the selectivity for C_2H_2 showed an opposite trend. The use of oxygen was found to provide a great enhancement of the plasma reforming of the simulated natural gas. For the combined plasma and partial oxidation in the reforming of CO_2-containing natural gas, air was found to be superior to pure oxygen in terms of reactant conversions, product selectivities, and specific energy consumption. The optimum conditions were found to be a hydrocarbons-to-oxygen feed molar ratio of 2/1 using air as an oxygen source, an applied voltage of 17.5 kV, and a frequency of 300 Hz, in providing the highest CH_4 conversion and synthesis gas selectivity, as well as extremely low specific energy consumption. The energy consumption was as low as 2.73×10^{-18} W s (17.02 eV) per molecule of converted reactant and 2.49×10^{-18} W s (16.60 eV) per molecule of produced hydrogen.

Keywords   Natural gas reforming · Gliding arc discharge · Plasma · Applied voltage · Input frequency · Partial oxidation

N. Rueangjitt · T. Sreethawong · S. Chavadej (✉)
The Petroleum and Petrochemical College, Chulalongkorn University, Soi Chula 12, Phyathai Road, Pathumwan, Bangkok 10330, Thailand
e-mail: sumaeth.c@chula.ac.th

Introduction

Non-thermal plasma chemistry is becoming increasingly interesting for a wide range of industrial applications because plasma chemical processing can be simply operated at near room temperature and atmospheric pressure, without the special requirements of pre-heating and post-cooling of the gas stream. The bulk gas temperature in the plasma zone normally remains close to room temperature, despite the much higher electron temperatures in the order of 10^4 K. Under the non-thermal plasma environment, the gas molecules are basically activated to create highly active species (electrons, ions, and free radicals) for both the initiation and the propagation of the chemical reactions. In industries and laboratories, different types of non-thermal plasmas that have long been employed both to effectively destroy several harmful chemicals and to selectively create a number of new useful chemicals include glow discharge, dielectric barrier discharge (DBD), corona discharge, microwave, and radio frequency (RF) plasmas [1]. Nevertheless, one major drawback of these conventional non-thermal plasmas is the low-energy plasma density, making it difficult for scaling up the reactor throughput. A gliding arc is a new discharge type of non-thermal plasma that successfully provides the most effective non-equilibrium characteristics with simultaneous high productivity and good selectivity [2]. In general, the gliding arc discharge was first designed and developed for use mostly in pollution control [3–8] and surface treatment [9–11]. In recent years, this plasma reactor type has received increasing interest in utilization for fuel conversion [12–18] and in applications for carbon black production [19, 20]. Some mathematical modeling studies were also investigated with an attempt to describe the physical characteristics and phenomena of the gliding arc discharge [21–26]. Intrinsically, the electrical parameters of the discharge are of great significance in influencing the electron energy distribution. A deep understanding of the effects of electrical parameters on the plasma behavior and reaction performance is the main key to manipulating the right electron number density and energy in generating active radical species which are necessarily favorable for any desired chemical reaction and product distribution. The optimal operating conditions are quite different in each plasma process and its applications, depending on plasma reactor type and configuration, feed composition, and target products [27].

In our previous work [28], the challenging concept of the direct utilization of raw natural gas with a high CO_2 content was investigated systematically. The study was carried out to observe the effect of feed gas components (CH_4, C_2H_6, C_3H_8, CO_2, and helium as the dilute gas) on natural gas reforming under non-thermal AC gliding arc discharge with the focus on the production of hydrogen and higher hydrocarbons at different feed flow rates. Interestingly, the preliminary results showed that the presence of other gas components in natural gas was found to significantly contribute to the synergistic effects on the overall reaction performance. The carbon dioxide present in the simulated natural gas markedly enhanced methane conversion, reduced coke formation, and lowered specific energy consumption. Several reports have revealed that the addition of oxygen to a CH_4-CO_2 feed gas mixture is one of the possible solutions for minimizing both the carbon formation and energy consumption for the CO_2 reforming reaction of methane [29–33]. Hence, in this present study, as the continuation of our previous work [28], the plasma reforming of CO_2-containing natural gas coupled with partial oxidation was investigated using gliding arc discharge at different voltages, frequencies, and hydrocarbons (HCs)-to-oxygen feed molar ratios. A comparative study between adding pure oxygen and adding air in the feed stream for the reforming of natural gas under gliding arc discharge was also conducted.

Experimental

Reactant Gases

Simulated natural gas containing methane, ethane, propane, and carbon dioxide, with a CH_4:C_2H_6:C_3H_8:CO_2 molar ratio of 70:5:5:20, was specially manufactured for this research by Thai Industry Gas (Public) Co., Ltd. Ultra-high purity oxygen and air zero, used for performing the plasma reforming of the simulated natural gas with partial oxidation, were also obtained from Thai Industry Gas (Public) Co., Ltd.

AC Gliding Arc Discharge System

The experimental set-up of the AC gliding arc discharge system is shown schematically in Fig. 1. The details of the gliding arc reactor configuration and the discharge system were described in the previous paper [28]. The gliding arc reactor is made of a glass tube with a 9 cm OD and an 8.5 cm ID, and has two diverging knife-shaped electrodes that were fabricated from stainless steel sheets with a 1.2 cm width for each electrode. The gap distance between the pair of electrodes was fixed at 6 mm. The flow rates of the reactant gases were regulated by a set of mass flow controllers and transducers supplied by SIERRA® Instrument, Inc. All of the reactant gases were well mixed in a mixing chamber before being introduced upward to the gliding arc reactor. The compositions of the feed gas mixture and the outlet gas were quantitatively analyzed by an on-line gas chromatograph (HP, 5890) equipped with two separate GC columns—a Carboxen 1000 packed column and a PLOT Al_2O_3 "S" capillary column—which are capable of detecting all hydrocarbons, CO, CO_2, H_2, O_2, and N_2.
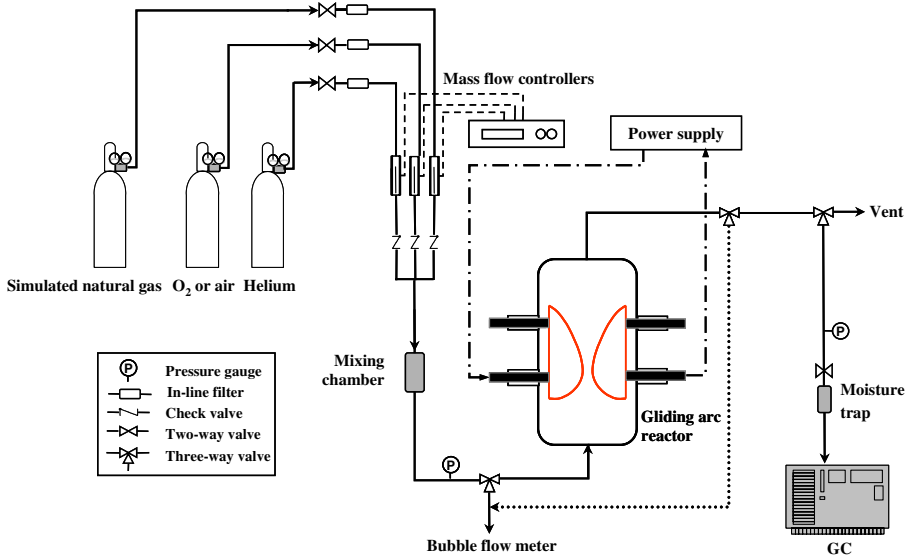

Fig. 1 Experimental set-up of the gliding arc plasma system

In order to determine the effects of applied voltage and input frequency on the CO_2-containing natural gas reforming, the gliding arc system was operated at various voltages and frequencies, while the feed flow rate and electrode gap distance were kept constant. The applied voltage and input frequency were adjusted by using a function generator. It should be noted that the voltage and current were measured at the low voltage side instead of at the high voltage side across the electrodes since the plasma generated is non-equilibrium in nature [28]. In addition, the optimum operational conditions obtained from the investigation of the effects of applied voltage and input frequency were used in the subsequent experiments of the combined plasma reforming and partial oxidation of the simulated CO_2-containing natural gas.

For any studied conditions, the feed gas mixture was first introduced into the gliding arc system without turning on the power supply unit. After the composition of outlet gas was invariant with time, it was turned on. The outlet gas composition was analyzed every 30 min by the on-line GC. After the system reached steady state, an analysis of outlet gas composition was taken at least a few times every hour. The experimental data were averaged to assess the process performance. During the experiments, the temperature at the reactor wall was found to be in the range of 150–200°C. Since the volume of the reactor outlet zone was rather large, the outlet gas was cooled close to room temperature. It was observed that a small amount of water droplets appeared on the surrounding inner wall of the gliding arc reactor during the experiments of the CO_2-natural gas reforming coupled with partial oxidation. In the case of using air, a NO_x analyzer was employed to determine if there were any nitrogen oxides present in the effluent gas; no nitrogen oxides were detected. Therefore, under the studied conditions, nitrogen oxides were not produced by the plasma system. The flow rates of both the feed and the outlet gases were measured by using a bubble flow meter because of the gas volume change after the reaction.

Reaction Performance Assessment

The reactant conversion is defined as:

$$\% \, \text{Reactant conversion} = \frac{(\text{Moles of reactant } in - \text{Moles of reactant } out)\,(100)}{\text{Moles of reactant } in} \quad (1)$$

The selectivities for C-containing products are defined on the basis of the amount of C-containing reactants converted into any specified product, as stated in Eq. 2. In the case of the hydrogen product, its selectivity is calculated based on H-containing reactants converted, as stated in Eq. 3:

$$\% \, \text{Selectivity for any hydrocarbon product} = [P](C_P)(100)/\Sigma[R](C_R) \quad (2)$$

where [P] = moles of product in the outlet gas stream; [R] = moles of each reactant in the feed stream to be converted; C_P = number of carbon atoms in a product molecule; C_R = number of carbon atoms in each reactant molecule

$$\% \, \text{Selectivity for hydrogen} = [P](H_P)(100)/\Sigma[R](H_R) \quad (3)$$

where H_P = number of hydrogen atoms in a product molecule; H_R = number of hydrogen atoms in each reactant molecule;

The product yield is formulated as follows:

$$\% \text{ C}_2 \text{ hydrocarbons yield } = \Sigma(\% \text{ CH}_4, \text{C}_2\text{H}_6, \text{C}_3\text{H}_8, \text{CO}_2 \text{ conversion}) \atop \Sigma(\% \text{ C}_2\text{H}_2, \text{C}_2\text{H}_4 \text{ selectivity})/(100) \tag{4}$$

$$\% \text{ H}_2 \text{ yield } = \Sigma(\% \text{ CH}_4, \text{C}_2\text{H}_6, \text{C}_3\text{H}_8 \text{ conversion})(\% \text{ H}_2 \text{ selectivity})/(100) \tag{5}$$

$$\% \text{ CO yield } = \Sigma(\% \text{ CH}_4, \text{C}_2\text{H}_6, \text{C}_3\text{H}_8, \text{CO}_2 \text{ conversion})(\% \text{ CO selectivity})/(100) \tag{6}$$

The specific energy consumption is calculated in a unit of W s per C-containing reactant molecule converted or per hydrogen molecule produced (W s/M) using the following equation:
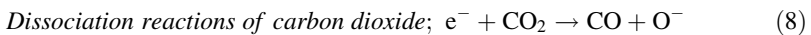
$$\text{Specific energy consumption } = (P)(60)/(\tilde{N})(M) \tag{7}$$

where P = power (W); $\tilde{N}$ = Avogadro's number $(6.02 \times 10^{23}$ molecules g mole$^{-1})$; M = rate of converted carbon in the feed or rate of produced hydrogen molecules (g mole min$^{-1})$
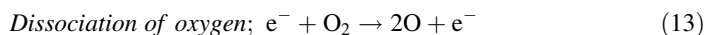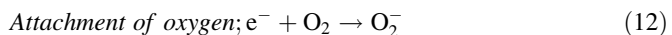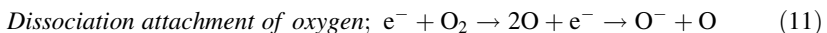
Results and Discussion

To provide a better comprehensive understanding of the plasma reforming reactions of CO_2-containing natural gas under AC non-thermal gliding arc discharge, both with and without partial oxidation, it is worth briefly describing all the possibilities of chemical pathways occurring under the studied conditions. In a plasma environment, high energy electrons generated by gliding arc discharge collide with the gaseous molecules of hydrocarbons and CO_2, creating a variety of chemically active radicals. In the absence of oxygen, the radicals of oxygen-active species are produced during the collisions between electrons and CO_2, as shown in Eqs. 8 and 9. Moreover, the produced CO can be further dissociated by the collisions with electrons to form coke and oxygen-active species (Eq. 10). In the case of added oxygen, a large amount of oxygen-active species can be produced from the collisions between electrons and oxygen molecules, as described by Eqs. 11–13. Eqs. 14–26 show the collisions between electrons and all hydrocarbons presented in the feed to produce hydrogen and various hydrocarbon species for subsequent reactions.
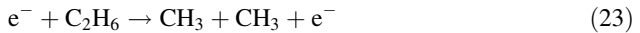
Electron–carbon dioxide collisions:

$$\textit{Dissociation reactions of carbon dioxide}; \ e^- + CO_2 \rightarrow CO + O^- \tag{8}$$

$$e^- + CO_2 \rightarrow CO + O + e^- \tag{9}$$

$$e^- + CO \rightarrow C + O + e^- \tag{10}$$

Electron–oxygen collisions:

$$\textit{Dissociation attachment of oxygen}; \ e^- + O_2 \rightarrow 2O + e^- \rightarrow O^- + O \tag{11}$$

$$\textit{Attachment of oxygen}; e^- + O_2 \rightarrow O_2^- \tag{12}$$
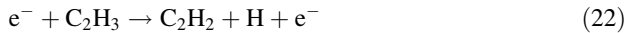
$$\textit{Dissociation of oxygen}; \ e^- + O_2 \rightarrow 2O + e^- \tag{13}$$

Electron–methane collisions:

$$e^- + CH_4 \rightarrow CH_3 + H + e^- \tag{14}$$

$$e^- + CH_3 \rightarrow CH_2 + H + e^- \tag{15}$$

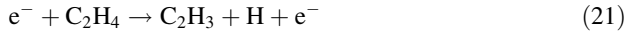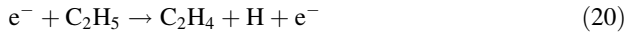$$e^- + CH_2 \rightarrow CH + H + e^- \tag{16}$$

$$e^- + CH \rightarrow C + H + e^- \tag{17}$$

$$H + H \rightarrow H_2 \tag{18}$$

Electron–ethane collision:

$$e^- + C_2H_6 \rightarrow C_2H_5 + H + e^- \tag{19}$$

$$e^- + C_2H_5 \rightarrow C_2H_4 + H + e^- \tag{20}$$

$$e^- + C_2H_4 \rightarrow C_2H_3 + H + e^- \tag{21}$$

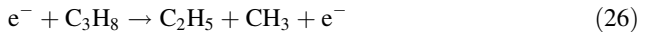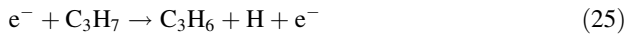$$e^- + C_2H_3 \rightarrow C_2H_2 + H + e^- \tag{22}$$

$$e^- + C_2H_6 \rightarrow CH_3 + CH_3 + e^- \tag{23}$$
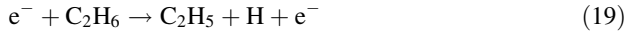
Electron–propane collision:

$$e^- + C_3H_8 \rightarrow C_3H_7 + H + e^- \tag{24}$$

$$e^- + C_3H_7 \rightarrow C_3H_6 + H + e^- \tag{25}$$

$$e^- + C_3H_8 \rightarrow C_2H_5 + CH_3 + e^- \tag{26}$$
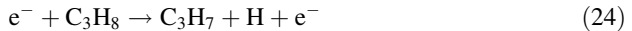
The oxygen-active species derived from CO_2 and O_2 can further extract hydrogen atoms from the molecules of hydrocarbon gases via the oxidative dehydrogenation reactions (Eqs. 27–39), consequently producing several chemically active radicals and water.
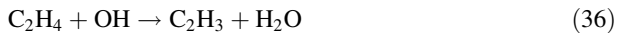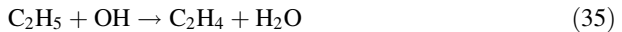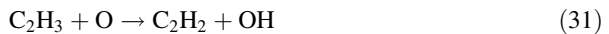
Oxidative dehydrogenation reactions:

$$CH_4 + O \rightarrow CH_3 + OH \tag{27}$$

$$C_2H_6 + O \rightarrow C_2H_5 + OH \tag{28}$$

$$C_2H_5 + O \rightarrow C_2H_4 + OH \tag{29}$$

$$C_2H_4 + O \rightarrow C_2H_3 + OH \tag{30}$$

$$C_2H_3 + O \rightarrow C_2H_2 + OH \tag{31}$$

$$C_3H_8 + O \rightarrow C_3H_7 + OH \tag{32}$$

$$CH_4 + OH \rightarrow CH_3 + H_2O \tag{33}$$

$$C_2H_6 + OH \rightarrow C_2H_5 + H_2O \tag{34}$$

$$C_2H_5 + OH \rightarrow C_2H_4 + H_2O \tag{35}$$

$$C_2H_4 + OH \rightarrow C_2H_3 + H_2O \tag{36}$$

$$C_2H_3 + OH \rightarrow C_2H_2 + H_2O \tag{37}$$

$$C_3H_8 + OH \rightarrow C_3H_7 + H_2O \tag{38}$$

$$C_3H_7 + OH \rightarrow C_3H_6 + H_2O \tag{39}$$

The C_2H_5, C_2H_3, and C_3H_7 radicals can further react to form ethylene, acetylene, and propene either by electron collision (Eqs. 21–23, 25 and 26) or by oxidative dehydrogenation reaction (Eqs. 29–31, 35–37, and 39). The extracted hydrogen atoms immediately form hydrogen gas according to Eq. 18. However, no propene was detected in the outlet
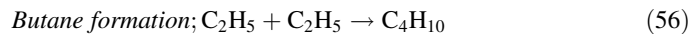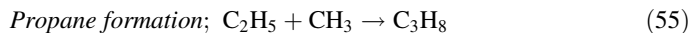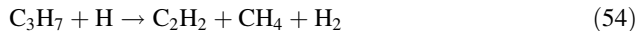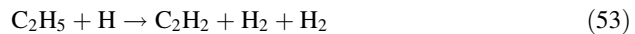
gas stream. It is therefore believed that the propene species was unstable and may probably undergo further reactions (Eqs. 40 and 41).

Propene hydrogenation and cracking reactions:

$$C_3H_6 + H_2 \rightarrow C_3H_8 \tag{40}$$

$$C_3H_6 \rightarrow C_2H_2 + CH_4 \tag{41}$$

Moreover, the radicals of hydrocarbons and hydrogen derived from the earlier reactions react further to combine with one another to form ethane, ethylene, acetylene, propane, and butane, as shown in Eqs. 42–57. In addition, ethane can be further dehydrogenated to form ethylene, while ethylene can also be dehydrogenated to form acetylene by either electron collision or oxidative dehydrogenation (Eqs. 19, 20, 28, 29, 34, and 35 for ethylene formation; and, Eqs. 21, 22, 30, 31, 36, and 37 for acetylene formation).

Coupling reactions of active species:

$$\textit{Ethane formation}; \ CH_3 + CH_3 \rightarrow C_2H_6 \tag{42}$$

$$C_2H_5 + H \rightarrow C_2H_6 \tag{43}$$

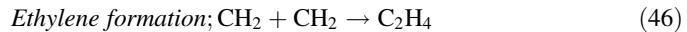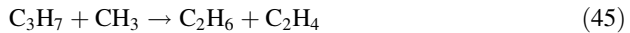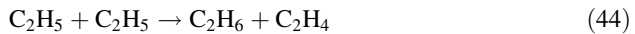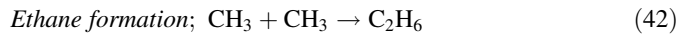$$C_2H_5 + C_2H_5 \rightarrow C_2H_6 + C_2H_4 \tag{44}$$

$$C_3H_7 + CH_3 \rightarrow C_2H_6 + C_2H_4 \tag{45}$$

$$\textit{Ethylene formation}; CH_2 + CH_2 \rightarrow C_2H_4 \tag{46}$$

$$CH_3 + CH_3 \rightarrow C_2H_4 + H_2 \tag{47}$$

$$C_2H_5 + H \rightarrow C_2H_4 + H_2 \tag{48}$$

$$C_3H_7 + H \rightarrow C_2H_4 + CH_4 \tag{49}$$

$$\textit{Acetylene formation}; \ CH + CH \rightarrow C_2H_2 \tag{50}$$

$$CH_2 + CH_2 \rightarrow C_2H_2 + H_2 \tag{51}$$

$$CH_3 + CH \rightarrow C_2H_2 + H_2 \tag{52}$$

$$C_2H_5 + H \rightarrow C_2H_2 + H_2 + H_2 \tag{53}$$

$$C_3H_7 + H \rightarrow C_2H_2 + CH_4 + H_2 \tag{54}$$

$$\textit{Propane formation}; \ C_2H_5 + CH_3 \rightarrow C_3H_8 \tag{55}$$

$$\textit{Butane formation}; C_2H_5 + C_2H_5 \rightarrow C_4H_{10} \tag{56}$$

$$C_3H_7 + CH_3 \rightarrow C_4H_{10} \tag{57}$$

Furthermore, a significant amount of CO and a very small amount of water were produced under the studied conditions, particularly in feed with high oxygen content. CO may be mainly formed via the partial oxidation reactions of the hydrocarbon reactants. Eqs. 58–62 show the partial oxidative pathways of methane to form CO and H_2 as the end products. The formation of water is believed to occur via the oxidative hydrocarbon reactions (Eqs. 33–39). In addition, water can be formed by the reactions between hydrogen or active hydrogen radical and active oxygen radical, as shown in Eqs. 63–65.

Carbon monoxide formation:

$$CH_3 + O \rightarrow HCHO + H \tag{58}$$

$$HCHO + O \rightarrow OH + CHO \tag{59}$$

$$CHO + O \rightarrow OH + CO \tag{60}$$

$$CHO + OH \rightarrow CO + H_2O \tag{61}$$

$$CHO + H \rightarrow H_2 + CO \tag{62}$$

Water formation:

$$2H + O \rightarrow H_2O \tag{63}$$

$$H_2 + O \rightarrow H_2O \tag{64}$$

$$H_2 + 1/2O \rightarrow H_2O \tag{65}$$

Additionally, hydrocarbon molecules may crack to form carbon and hydrogen via thermal cracking reactions (Eqs. 66–68).

$$CH_4 \rightarrow C + 2H_2 \tag{66}$$

$$C_2H_6 \rightarrow 2C + 3H_2 \tag{67}$$

$$C_3H_8 \rightarrow 3C + 4H_2 \tag{68}$$

Effect of Applied Voltage

Typically, the composition and type of gases used as a feed mixture are of considerable importance to affect the plasma characteristics (i.e., breakdown voltage, electrical conductivity, and physical appearance) and the plasma stability owing to the different properties of each gas component. Applied voltage is one of the most key operating parameters in controlling the non-thermal plasma performance and the chemical reaction pathways. In this study, the effect of applied voltage was firstly investigated by varying it while the feed flow rate, frequency, and electrode gap distance were kept constant at 125 cm^3/min, 300 Hz, and 6 mm, respectively, which were the optimum conditions obtained from the previous work [28].

Figure 2(a) shows the results of reactant conversions and product yields as a function of applied voltage. As expected, the conversions of all reactants in the CH$_4$/C$_2$H$_6$/C$_3$H$_8$/CO$_2$ feed were obviously enhanced by increasing the applied voltage from 12.5 to 21.5 kV. The yields of H$_2$ and C$_2$ products were found to be improved remarkably at higher applied voltages. In this plasma system, the highest operating applied voltage of 21.5 kV was limited by the formation of a coke filament between the two electrodes during a relatively short operation period, which caused instability and thereby permanent extinction in the plasma, whereas the lowest operating applied voltage of 12.5 kV was limited by the breakdown voltage, which is the minimum value of voltage required to create the steady plasma environment. Basically, an increase in voltage applied to the plasma-chemical reactions contributes directly to a stronger electric field strength across the electrodes. More specifically, the electric field strength is simply proportional to the mean electron energy and electron temperature in the plasma. That is, at a higher voltage, the plasma generated exhibits not only electrons with a higher average energy and temperature but also a higher electron density, as indicated in terms of a higher current, which will be discussed later. For this reason, in non-thermal plasma, the opportunity for the occurrence
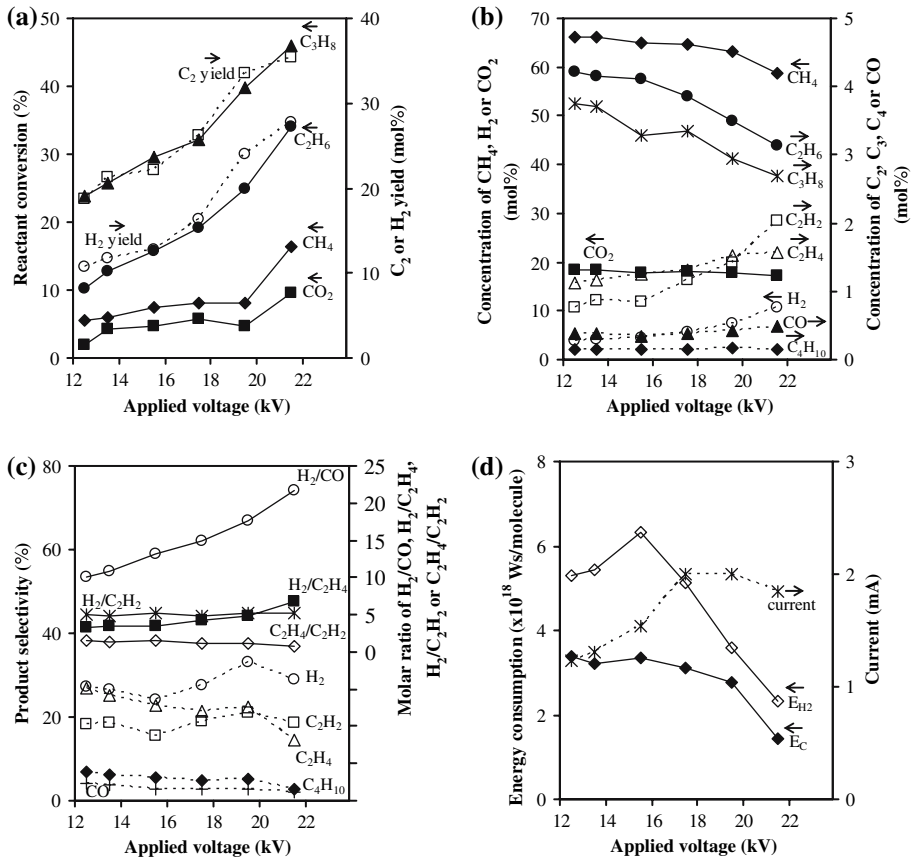
Fig. 2 Effect of applied voltage on (**a**) reactant conversions and product yields, (**b**) concentrations of outlet gas, (**c**) product selectivities and product molar ratios, and (**d**) specific energy consumption and current of the simulated CO_2-containing natural gas reforming (feed flow rate, 125 cm^3/min; frequency, 300 Hz; and, electrode gap distance, 6 mm) (E_{H2}: energy per H_2 molecule produced; E_C: energy per reactant molecule converted)

of elementary chemical reactions with electron impact (mainly ionization, excitation, and dissociation of gas molecules) is improved, leading to an increasing number of chemically reactive species being formed to activate the plasma-chemical reactions. The present results are in agreement with literature [18, 34, 35].

Figure 2(b) shows the main products (C_2H_4, C_2H_2, and H_2) under the studied conditions. In the applied voltage range of 12.5–15.5 kV, the concentrations of H_2, C_2H_2, C_2H_4, C_4H_{10}, and CO appeared only slightly changed, but in the range of 15.5–21.5 kV, increasing applied voltage remarkably increased the concentrations of H_2, C_2H_2, and C_2H_4, with only small changes in C_4H_{10} and CO concentrations. By considering the applied voltage range of 15.5–21.5 kV, the concentration of C_2H_2 increased more sharply than that of C_2H_4, which in turn resulted in a higher concentration of C_2H_2 than C_2H_4 at an applied voltage above 19.5 kV. According to the earlier explanation for the physical plasma behavior, the influence of stronger electric field or greater electron number density causes the promotion of inelastic collisions between reacting gas molecules and energetic electrons (Eqs. 8–10 and 14–26), therefore leading directly to the increase in conversions of

CH_4, C_2H_6, C_3H_8, and CO_2, as well as the product formation. Moreover, the increasing C_2H_2 and the decreasing C_2H_4 with increasing applied voltage suggest that the dehydrogenation (Eqs. 21, 22, 30, 31, 36 and 37) can be enhanced greatly at a very high applied voltage, especially greater than 20 kV. It is worth noting that hydrocarbons containing a carbon number greater than C_4 could not be detected in the studied range of applied voltage. In addition, from the Raman analysis, the deposited material on the electrode surface was found to contain only pure carbon. These suggest that the studied gliding arc system is not suitable for producing higher hydrocarbons ($> C_4$) from natural gas.

Figure 2(c) shows the influence of applied voltage on the product selectivities and molar ratios of products. The selectivities for both H_2 and C_2H_2 tended to slightly increase with increasing applied voltage up to 19.5 kV. After that, in the range of 19.5–21.5 kV, they did not further increase but conversely dropped sharply. In contrast to the selectivities for H_2 and C_2H_2, those for C_2H_4, C_4H_{10}, and CO progressively declined with increasing applied voltage from 12.5 to 21.5 kV; particularly noticeable was that for C_2H_4. The result can be explained in that at higher applied voltages, more energetic electrons, as well as O active species dissociated from CO_2 and CO (Eqs. 8–10), essentially participate in the encouragement of the plasma-chemical dehydrogenation of hydrocarbon species (e.g. C_2H_4 and C_2H_6) for being converted into smaller molecules (e.g. H_2 and C_2H_2) according to Eqs. 19–23, 28–31, and 34–37, which is more dominant over their coupling reactions (Eqs. 42–57). By considering the applied voltage range of 19.5–21.5 kV, the decreases in the H_2 and C_2H_2 selectivities against the applied voltage is mainly caused by a tremendously increasing amount of carbon formed on the electrode surface, about two times greater at the high applied voltage of 21.5 kV (15.3% of carbon) as compared to that at 19.5 kV (7.2% of carbon), noting that the amount of carbon was given from the calculation of carbon balance. With increasing applied voltage, the CO selectivity slightly decreased and the molar ratio of H_2/CO increased significantly, suggesting that the increase in the applied voltage leads to not only more CO_2 dissociation (Eqs. 8 and 9) but also to more CO dissociation ($e^- + CO \rightarrow C + O + e^-$), as shown in Eq. 10. Therefore, the CO formation subsequently decreased. With an increasing of the applied voltage from 12.5 to 21.5 kV, the apparent increase in the H_2/CO molar ratio from approximately 10–22 can be explained in that both the dehydrogenation reactions (Eqs. 14–22, 24, 25, and 27–39) and the direct thermal cracking of hydrocarbons to produce H_2 and carbon (Eqs. 66–68) have a higher possibility to occur, as compared to the CO_2 dissociation, since the dissociation energy of CO_2 is higher than those of CH_4, C_2H_6, and C_3H_8.

Figure 2(d) shows that a higher current is generated by increasing the applied voltage, representing a larger number of energetic electrons produced. It is worth noting that a higher current induces higher concentrations of active gaseous species available to react and form new chemical species. Additionally, Fig. 2(d) shows the energy consumption as a function of applied voltage. The consumed energy for converting a hydrocarbon reactant molecule or producing a hydrogen molecule drastically decreased at particularly high applied voltages. Clearly, the minimum energy consumption was found to correspond to the highest applied voltage of 21.5 kV in this studied system. These results can be explained by the increases in the reactant conversions and hydrogen production, when the applied voltage was increased, thus reducing the specific energy consumption of the system. As mentioned before, with an applied voltage greater than 21.5 kV, the system was not able to operate because of a greater amount of carbon deposit on the electrode surfaces and on the inner reactor glass wall, which results from the dissociation and the cracking reactions due to high temperatures in the plasma zone, causing instability of the plasma. From the results, an applied voltage of 17.5 kV was selected for further investigation

because the plasma feature was found to be apparently more stable than that at higher applied voltages, and it would give a relatively good plasma-reaction performance, including high reactant conversions, high product yields and selectivities, and relatively low energy consumption.

Effect of Input Frequency

For the investigation of the effect of input frequency on the reforming reactions of the simulated natural gas, the frequency parameter was experimentally varied in the range of 250–700 Hz. In operating the AC gliding arc discharge system in this study, the highest operating frequency (700 Hz) was limited by the unstable gliding arc discharge, observed from the discharge appearance and its behavior (e.g. an extremely small number of arcs produced with unsmooth arc patterns along the knife-shaped electrode pairs), whereas the lowest operating frequency (250 Hz) was limited by the coke formation on the electrodes, causing a disturbance of the gliding arc discharge path and a sharp increase in current.

   The effects of frequency on the CH_4, C_2H_6, C_3H_8, and CO_2 conversions, as well as the H_2 and C_2 yields, are presented in Fig. 3(a). The results show that the increase in the frequency led to the decrease in the reactant conversions and product yields, which is in contrast to the effect of applied voltage. Sreethawong et al. [18] also reported that both the CH_4 and O_2 conversions decreased as the frequency increased in the investigation of the partial oxidation of methane using the multistage gliding arc discharge system. The conversions for all reactants were in the following order: $C_3H_8 > C_2H_6 > CH_4 > CO_2$, resulting from their bond dissociation energies, which are 4.33, 4.35, 4.55, and 5.52 eV, respectively, as mentioned in our previous work [28]. The concentrations of products (C_2, H_2, and CO) also gradually declined with increasing frequency, as illustrated in Fig. 3(b). In an alternating current discharge system, due to the reversal in polarity of the electric field, each electrode acts alternately as an anode and cathode, and the current periodically reverses in direction. A faster reversal in electric field at a higher frequency causes a slower decay rate of space charges (electrons and ions) [18, 37–38]. For this reason, at a constant applied voltage and a fixed electrode gap distance, the electric current needed to initiate and maintain the discharge plasma is reduced with increasing frequency. Consequently, at a higher frequency, the lower the current or numbers of electrons, the lower the number of reactive species to activate the plasma-chemical reactions. Based on the basic concept of the frequency effect as stated, the space charge characteristic of the alternating current discharge is the influential factor of frequency in changing the behaviors of discharge and the reaction performance. Again, increasing frequency adversely brings about the reduction in the number of electrons generated for initiating the chemically reactive species via the elementary processes with electron impact and for activating the subsequent chemical reactions, resulting in lower conversions and product yields. Additionally, with increasing the frequency, the fewer number of electrons generated in the discharge zone can certainly be confirmed by the decrease in the measured current against the frequency (which will be discussed later).

   Figure 3(c) shows the product selectivities as a function of frequency. Within the low frequency range of 250–500 Hz, both H_2 and C_2H_2 selectivities moderately dropped when the frequency increased, and then approached the minimum values at a frequency of 500 Hz. This result indicates that the electron collisions (Eqs. 14–22, 24 and 25) and oxidative dehydrogenation reactions (Eqs. 27–39) become significantly dominant at low frequency. Afterwards, within the higher frequency range of 500–700 Hz, the two
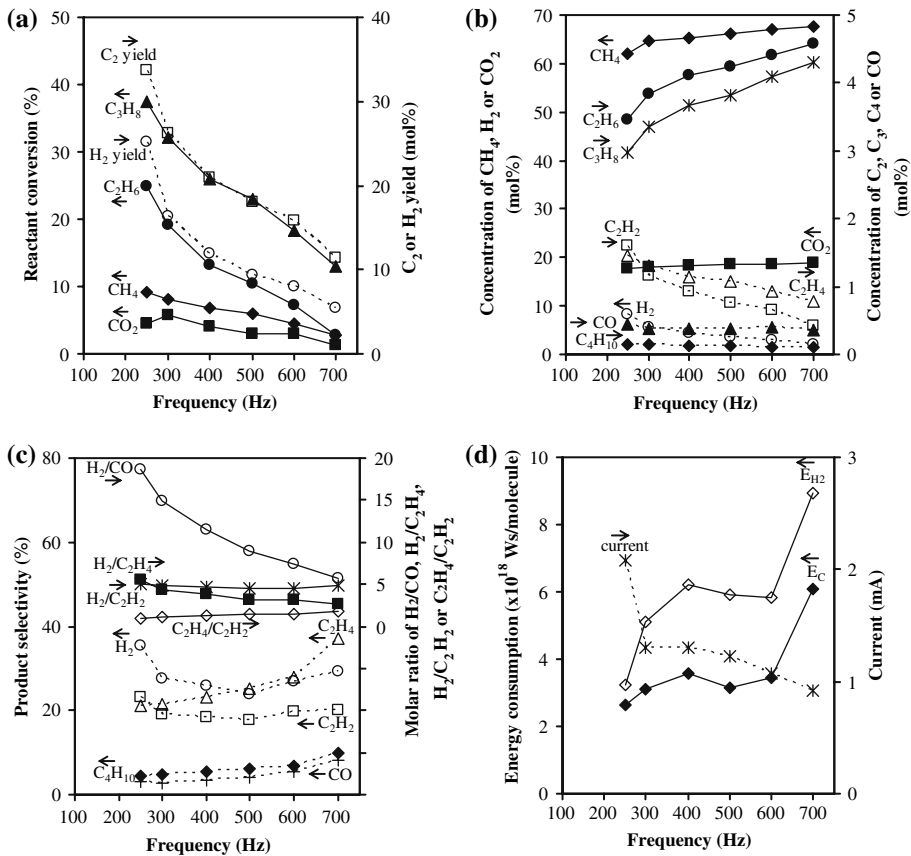
Fig. 3 Effect of input frequency on (**a**) reactant conversions and product yields, (**b**) concentrations of outlet gas, (**c**) product selectivities and product molar ratios, and (**d**) specific energy consumption and current of the simulated CO_2-containing natural gas reforming (feed flow rate, 125 cm^3/min; applied voltage, 17.5 kV; and, electrode gap distance, 6 mm) (E_{H2}: energy per H_2 molecule produced; E_C: energy per reactant molecule converted)

selectivities increased slightly with increasing frequency. Beyond 500 Hz, the coupling reactions of radicals (Eqs. 50–54) to form the C_2H_2 product is more favorable. The C_2H_4, C_4H_{10}, and CO selectivities correspondingly increased with increasing frequency within the whole studied range, suggesting that the promotion of coupling reactions (Eqs. 42–57) can be attained by increasing the frequency. The CO selectivity increased with increasing frequency, while the CO concentration in the produced gas slightly decreased, typically due to a smaller amount of electrons being available to interact with CO for further reactions.

Figure 3(d) shows decreasing current with increasing frequency. Moreover, Fig. 3(d) also shows the effect of frequency on the specific energy consumption based on both reactants converted and hydrogen produced. Contrary to the results of increasing applied voltage (Fig. 2(d)), at a higher frequency, the system required higher energy for converting the reactants and producing the hydrogen. This is possibly due to the decrease in quantities of converted reactants and produced hydrogen when the frequency increases. It should also

be noted that, with increasing frequency, the intensity of the arc generated between the electrodes was observed to be reduced. This is presumably because the larger number of sine-waveform cycles per second (higher frequency) may require higher input energy to sufficiently sustain the gliding arc discharge, thereby reducing the intensity of the produced arc.

From the experimental results, the highest reactant conversions, the good selectivities, and the lowest power consumption were achieved at a frequency of 250 Hz. Even though at 250 Hz there was comparatively somewhat better reaction performance, the system was found to be unstable as a result of the coke deposit. Hence, 300 Hz was selected as the optimum frequency for the further investigation of the effects of adding oxygen on the reforming of the simulated CO_2-containing natural gas.

Effect of Oxygen Addition

For the combined plasma reforming and partial oxidation of the simulated natural gas, the effect of hydrocarbons-to-oxygen (HCs/O_2) feed molar ratio was investigated to determine whether or not the addition of oxygen to the natural gas feed improved the system performance by using two different oxygen sources: pure oxygen and air. In addition, the results of CO_2-containing natural gas reforming with and without partial oxidation were compared in order to obtain better clarification of the effects of oxygen on the plasma reforming reactions of natural gas. To observe the effects of adding oxygen, the studied plasma system was operated at different HCs/O_2 feed molar ratios, a feed flow rate of 125 cm^3/min, an applied voltage of 17.5 kV, a frequency of 300 Hz, and an electrode gap distance of 6 mm. The results of the combined plasma reforming and partial oxidation under different HCs/O_2 feed molar ratios are presented in Figs. 4–8. The molar ratios of HCs/O_2 in the feed were varied from 2/1 to 20/1, using either pure oxygen or air, whereas the HCs/O_2 molar ratio of 1/0 represents the condition of no oxygen in feed. In this study, a HCs/O_2 molar ratio lower than 2/1 was not investigated since it is close to the upper explosion limit.

Fig. 4 Effect of HCs/O_2 feed molar ratio on reactant conversions of the simulated CO_2-containing natural gas reforming using feeds with pure oxygen (solid lines) and air (dotted lines) added, and feed in the absence of oxygen (feed flow rate, 125 cm^3/min; applied voltage, 17.5 kV; frequency, 300 Hz; and, electrode gap distance, 6 mm)
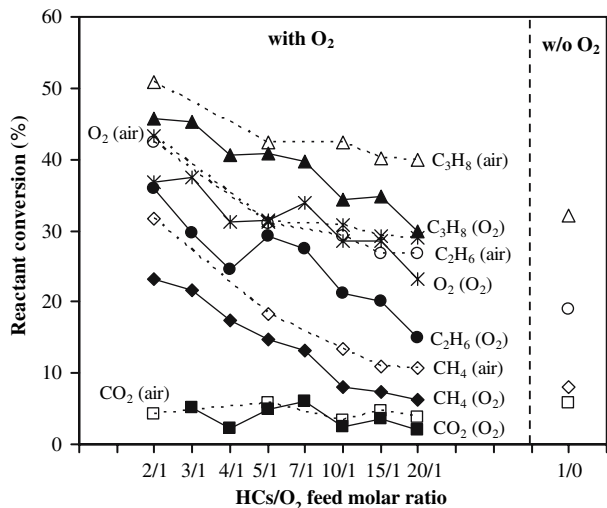
Fig. 5 Effect of HCs/O_2 feed molar ratio on product yields of the simulated CO_2-containing natural gas reforming using feeds with pure oxygen (solid lines) and air (dotted lines) added, and feed in the absence of oxygen (feed flow rate, 125 cm^3/min; applied voltage, 17.5 kV; frequency, 300 Hz; and, electrode gap distance, 6 mm)
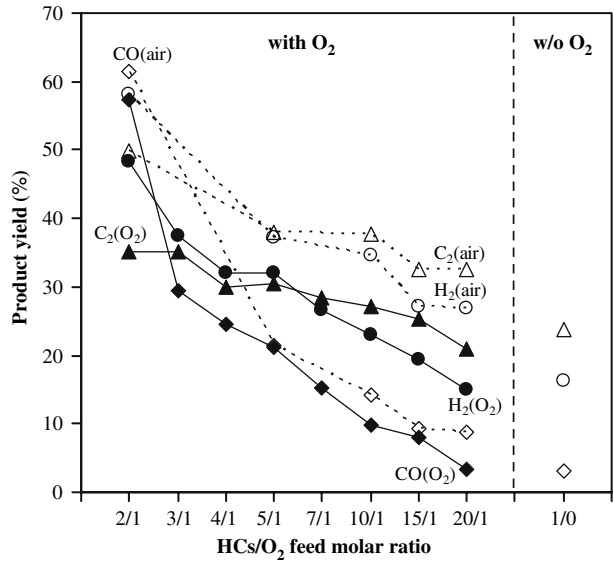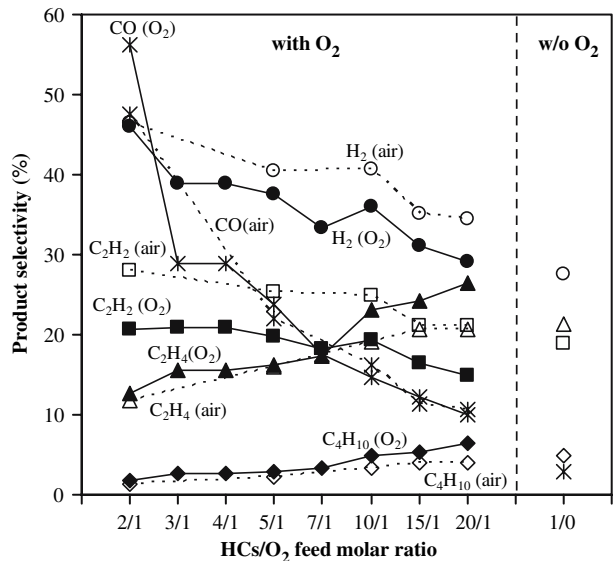

Fig. 6 Effect of HCs/O_2 feed molar ratio on product selectivities of the simulated CO_2-containing natural gas reforming using feeds with pure oxygen (solid lines) and air (dotted lines) added, and feed in the absence of oxygen (feed flow rate, 125 cm^3/min; applied voltage, 17.5 kV; frequency, 300 Hz; and, electrode gap distance, 6 mm)

As shown in Figs. 4 and 5, the conversions of all reactants, except CO_2, as well as the product yields, increase substantially with decreasing HCs/O_2 molar ratio when either air or pure oxygen is added over the whole studied range of HCs/O_2 ratios. In comparisons between these two oxygen sources, air provided a higher process performance in terms of both reactant conversion and product yield. The results reveal that the addition of air in the feed, even a very small amount, potentially contributes the positive effect to the activation of reactant gases for the CO_2-containing natural gas reforming. For the case of pure oxygen addition, the improvement of reaction performance is attained when the feed molar ratio of HCs/O_2 was kept below 15/1. From Figs. 6 and 7, the comparisons of the results of product

Fig. 7 Effect of HCs/O_2 feed molar ratio on product molar ratios of the simulated CO_2-containing natural gas reforming using feeds with pure oxygen (solid lines) and air (dotted lines) added, and feed in the absence of oxygen (feed flow rate, 125 cm^3/min; applied voltage, 17.5 kV; frequency, 300 Hz; and, electrode gap distance, 6 mm)
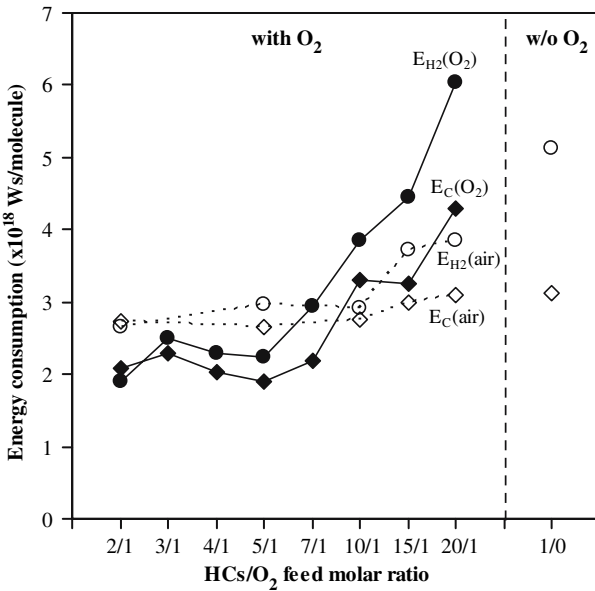
Fig. 8 Effect of HCs/O_2 feed molar ratio on energy consumption of the simulated CO_2-containing natural gas reforming using feeds with pure oxygen (solid lines) and air (dotted lines) added, and feed in the absence of oxygen (feed flow rate, 125 cm^3/min; applied voltage, 17.5 kV; frequen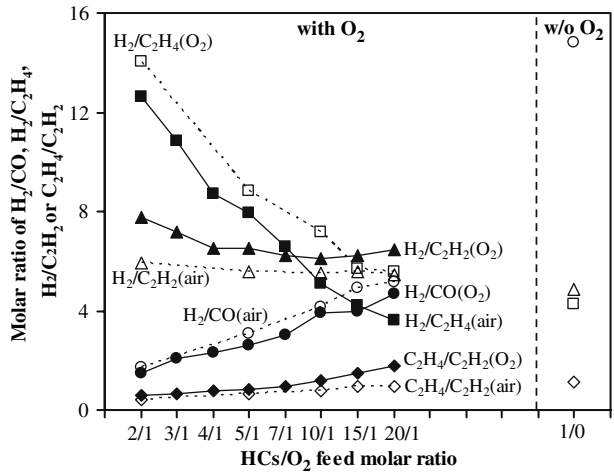cy, 300 Hz; and, electrode gap distance, 6 mm) (E_{H2}: energy per H_2 molecule produced; E_C: energy per reactant molecule converted)

selectivity and molar ratio reveal that the selectivities for CO and H_2 of the feed with adding oxygen (both air and pure oxygen) were higher than the ones of the feed without adding oxygen, particularly at a low HCs/O_2 ratio with a high O_2 content, indicating that the synthesis gas production is likely to increase with adding oxygen to natural gas. Regarding the comparative results of energy consumption shown in Fig. 8, much less energy was consumed for converting reactants and producing hydrogen in the case of the feed with air and pure oxygen added as compared to the feed without adding oxygen.

Moreover, the amount of coke formed during the operation was outstandingly minimized when some oxygen was added into the natural gas feed. Again, the results suggest that the addition of oxygen can provide benefits in the reduction of both energy consumption and coke deposition. From these comparative results, it can be concluded that the addition of oxygen into the feed provides synergistic effects on the CO_2-containing natural gas reforming with not only higher reactant conversions, product yields, and selectivities, but also lower energy consumption.

Apart from the significant process improvement by the addition of oxygen as mentioned above, the effects of HCs/O_2 feed molar ratio on the overall performance of plasma reactions are further discussed here. As can be seen from Figs. 4 and 5, for both cases of feeds, pure oxygen and air, increasing the feed molar ratio of HCs/O_2 resulted in significant decreases of all reactant conversions and product yields. The reduction of conversions and yields at high HCs/O_2 molar ratios is certainly due to the fact that a decrease of O_2 content at higher HCs/O_2 molar ratios results in less probability of extracting H atoms from the hydrocarbon molecules by the O active species primarily generated from the electron collision (Eqs. 11–13), leading to the decreases in CH_4, C_2H_6, and C_3H_8 conversions according to Eqs. 27–39. In the presence of oxygen, oxygen molecules are activated by plasma and subsequently provide a source of chemically oxygen-active species formed via the three possible pathways, as stated in Eqs. 11–13 [18, 36–37].

It should be noted that, in Fig. 4, the result of CO_2 conversion is not included for the case of adding pure oxygen to the feed at the lowest HCs/O_2 molar ratio of 2/1 due to the minus sign of the CO_2 conversion. The negative CO_2 conversion can be explained in that the formation rate of CO_2 by the hydrocarbon oxidation is higher than the CO_2 consumption rate by the reforming reactions [33]. Both H_2 and C_2 yields increase substantially with a decreasing HCs/O_2 molar ratio when the HCs/O_2 molar ratio is lower than 5/1 for both cases of pure oxygen and air, as shown in Fig. 5. The H_2 yield was found to be higher than the C_2 yield in the HCs/O_2 range of 2/1–5/1; conversely the C_2 yield became higher than the H_2 yield beyond the HCs/O_2 ratio of 5/1 for both cases, pure oxygen and air. Therefore, the HCs/O_2 molar ratio at 5/1 is regarded as a turning point, indicating that H_2 production via the dehydrogenation reactions (Eqs. 14–39) more favorably occurs than C_2 production via the coupling reactions (Eqs. 42–54) under high O_2 content conditions (HCs/O_2 molar ratio <5/1), while the coupling reactions for producing C_2 hydrocarbons are more favorable under low O_2 content conditions (HCs/O_2 molar ratio >5/1). In a comparison between pure oxygen and air, at any given HCs/O_2, all hydrocarbon conversions and product yields when adding air were higher than those when adding pure oxygen, while the CO_2 and O_2 conversions, as well as the CO yield, were relatively similar. These results may suggest that the presence of nitrogen, the major gas component in air, is probably responsible for promoting the plasma-chemical reactions by acting as a third body in the reaction to receive the excessive energy of the products and making them stable, although the concentration of gas components in simulated natural gas is diluted when using air instead of pure oxygen. The present results are in good agreement with previous work reporting that using nitrogen as an additive gas provides a positive effect on methane conversion by the excitation of the nitrogen molecule into a higher vibrational level and meta-stable state [16].

Figure 6 shows the effect of the HCs/O_2 feed molar ratio on the product selectivities. For both cases, i.e. pure oxygen and air, the selectivities for C_2H_4 and C_4H_{10} remarkably increased with increasing HCs/O_2 molar ratio from 2/1 to 20/1, whereas the selectivities for H_2 and C_2H_2 slightly decreased. Interestingly, the CO selectivity abruptly decreased as the HCs/O_2 molar ratio increased. At a high HCs/O_2 molar ratio, less availability of O active

species is responsible for less opportunity for dehydrogenation reactions (Eqs. 14–39) to produce H_2 and small hydrocarbon molecules (C_2H_2), as well as CO formation via the reactions in Eqs. 58–62. Conversely, the opportunity for coupling reactions to form larger hydrocarbon molecules (C_2H_4 and C_4H_{10}) is more favorable at higher HCs/O_2 molar ratios (Eqs. 46–49, 56, and 57). This explanation is also confirmed from the results of the increasing H_2/CO and C_2H_4/C_2H_2 molar ratios together with decreasing H_2/C_2H_2 molar ratio, as shown in Fig. 7. At a HCs/O_2 feed molar ratio of 2/1 using either pure oxygen or air, the ratio of H_2/CO was observed to be nearly 2, corresponding to the theoretical stoichiometric ratio for the partial oxidation of methane, which is the primary gas component in the simulated natural gas feed. As also reported by Supat et al. [38], the H_2/CO ratio was found to be 2.2 at a CH_4/O_2 ratio of 2/1 for the partial oxidation of methane with air using corona discharge. By increasing the HCs/O_2 ratio from 2/1 to 20/1, the H_2/CO ratio increased to about 5 at the maximum HCs/O_2 ratio of 20/1 since the CO formation abruptly dropped (see Fig. 6). As shown in Fig. 6, the H_2 and C_2H_2 selectivities seem to be higher in the case of adding air throughout the studied range of HCs/O_2 ratios, while the higher C_2H_4 and C_4H_{10} selectivities can be clearly seen in the case of adding pure oxygen at high HCs/O_2 ratios of above 7/1. However, the CO selectivity in both cases was nearly the same. These results imply that a higher probability of the dehydrogenation of hydrocarbons (Eqs. 14–39) is obtained in the case of adding air, but a higher probability of coupling reactions (Eqs. 42–57) is preferentially obtained in the case of adding pure oxygen. As confirmed by the product molar ratios in Fig. 7, the H_2/C_2H_2 ratio in the case of adding air is lower than that when adding pure oxygen. Oppositely, however, the H_2/C_2H_4 ratio when adding air was higher than when adding pure oxygen, suggesting that the dehydrogenation of C_2H_4 to C_2H_2 (Eq. 21, 22, 30, 31, 36, and 37) in the case of adding air is much more favorable than in the case of adding oxygen. This also resulted in the lower C_2H_4/C_2H_2 ratio when adding air.

Figure 8 shows the energy consumption for converting reactants and for producing hydrogen at different HCs/O_2 feed molar ratios. At HCs/O_2 molar ratios between 2/1 and 5/1, very low energy consumption was attained in both cases, i.e. using pure oxygen and air, and there was no significant difference in the energy consumption in this range of molar ratios. Beyond a HCs/O_2 molar ratio of 5/1, the energy consumption increased sharply with further increasing HCs/O_2 molar ratio from 5/1 to 20/1, particularly in the case of using pure oxygen, mainly due to the decreases in both converted reactant and produced hydrogen. These results suggest that the energy consumption in the plasma reforming of simulated natural gas with partial oxidation can be significantly reduced by adding oxygen. Moreover, a decreased tendency for coke deposition on the electrode surface and inner reactor glass wall can be obtained at lower feed molar ratios (with a high O_2 content). Energy consumption was also experimentally found to be lower in the case of adding air as compared to adding pure oxygen, especially in the HCs/O_2 molar ratio range of 10/1–20/1. The present results suggest that the addition of oxygen in the form of air can provide a reduction of both energy consumption and coke deposition.

Conclusions

In the AC gliding arc discharge system used in this study, both applied voltage and input frequency were found to be very important electrical parameters, affecting the stabilization of the gliding arc discharge phenomena and the plasma-chemical activation of natural gas reforming. The effects of both applied voltage and frequency significantly affected the

reactant conversions, product selectivities, and product yields for the reforming of the simulated natural gas containing a high CO_2 content, largely due to the alteration of electric field characteristics within the discharge zone. A high applied voltage and a low input frequency are required to attain high H_2 and hydrocarbon yields. However, under an intensive current condition in the reforming of natural gas, coke formation on the surface of the electrodes appeared and caused a plasma disturbance in the gliding arc system. The introduction of a small amount of oxygen to the simulated natural gas was found to be a very effective means to minimize the carbon deposit on the electrode surface and inner reactor wall, as well as to improve the performance of CO_2-containing natural gas reforming in terms of reactant conversion, product yield, product selectivity, and energy consumption. Using air in the combined CO_2-containing natural gas reforming with partial oxidation provides better process performance than using pure oxygen because the nitrogen in the air enhances the plasma reforming reactions.

References

1. Eliasson B, Kogelschatz U (1991) IEEE T Plasma Sci 19:1063–1077
2. Fridman A, Kennedy LA (2004) Plasma physics and engineering. Taylor & Francis, New York
3. Indarto A, Choi JW, Lee H, Song HK, Coowanitwong N (2006) Plasma Devices Oper 14:15–26
4. Krawczyk K, Młotek M (2001) Appl Catal B Environ 30:233–245
5. Moussa D, Brisset JL, Hazard J (2003) Mater 102:189–200
6. Abdelmalek F, Gharbi S, Benstaali B, Addou A, Brisset JL (2004) Water Res 38:2339–2347
7. Moreau M, Orange N, Brisset JL (2005) Ozone Sci Eng 27:469–473
8. Burlica R, Kirkpatrick MJ, Locke BR (2006) J Electrostat 64:35–43
9. Janča J, Czernichowski A (1998) Surf Coat Tech 98:1112–1115
10. Janca J, Stahel P, Buchta J, Subedi D, Krcma F, Pryckova J (2001) Plasmas Polym 6:15–26
11. Benstaali B, Addou A, Brisset JL (2002) Mater Chem Phys 78:214–221
12. Czernichowski A (2001) Oil Gas Sci Technol 56:181–198
13. Rusu I, Cormier JM (2003) Chem Eng J 91:23–31
14. Indarto A, Choi JW, Lee H, Song HK (2005) J Nat Gas Chem 14:13–21
15. Paulmier T, Fulcheri L (2005) Chem Eng J 106:59–71
16. Indarto A, Choi JW, Lee H, Song HK (2006) Energy 31:2986–2995
17. Holmen A, Olsvik O, Rokstad OA (1995) Fuel Process Technol 42:249–267
18. Sreethawong T, Thakonpatthanakun P, Chavadej S (2007) Int J Hydrogen Energ 32:1067–1079
19. Zielinski T, Kijenski J (2005) Compos Part A Appl S 36:467–471
20. Opalińska T, Zieliński T, Schmidt-Szalowski K (2003) Polish J Chem 77:1357–1361
21. Fridman A, Naster S, Kennedy LA (1999) Prog Energ Combust 25:211–231
22. Yardimci OM, Savelier AV, Fridman AA, Kennedy LA (2000) J Appl Phys 87:1632–1641
23. Kuzunetsova IV, Kalashnikov NY, Gutsol AF, Fridman AA, Kennedy LA (2002) J Appl Phys 92: 4231–4237
24. Richard F, Cormier JM, Pellerin S (1996) J Appl Phys 79:2245–2250
25. Pellerin S, Richard F, Chapelle J, Cormier J-M, Musiol K (2000) J Phys D: Appl Phys 33:2407–2419
26. Pellerin S, Cormier JM, Richard F, Musiol K, Chapelle J (1999) J Phys D: Appl Phys 32:891–897
27. Napartovich AP (2001) Plasmas Polym 6:1–14
28. Rueangjitt N, Akarawitoo C, Sreethawong T, Chavadej S (2007) Plasma Chem Plasma Process 27: 559–576
29. Liu S, Xiong G, Dong H, Yang W (2000) Appl Catal A Gen 202:141–146
30. Larentis AL, de Resende NS, Salim VMM, Pinto JC (2001) Appl Catal A: Gen 215:211–224
31. Souza MMVM, Schmal M (2003) Appl Catal A: Gen 255:83–92

32. O'Connor AM, Ross JRH (1998) Catal Today 46:203–210
33. Jing QS, Fei JH, Lou H, Mo LY, Zheng XM (2004) Energ Convers Manage 45:3127–3137
34. Thanyachotpaiboon K, Chavadej S, Caldwell L, Lobban LL, Mallinson RG (1998) AIChE J 44: 2252–2257
35. Chavadej S, Supat K, Lobban LL, Mallinson RG (2005) J Chem Eng Jpn 38:163–170
36. Liu CJ, Marafee A, Hill B, Xu GH, Mallinson RG, Lobban LL (1996) Ind Eng Chem Res 35:3295–3301
37. Supat K, Chavadej S, Lobban LL, Mallinson RG (2003) Ind Eng Chem Res 42:1654–1661
38. Supat K, Kruapong A, Chavadej S, Lobban LL, Mallinson RG (2003) Energ Fuel 17:474–481